First principles study of the structural, electronic, and transport properties of triarylamine-based nanowires

Akinlolu Akande, Sandip Bhattacharya, Thomas Cathcart, and Stefano Sanvito

Citation: The Journal of Chemical Physics **140**, 074301 (2014); doi: 10.1063/1.4864754
View online: http://dx.doi.org/10.1063/1.4864754
View Table of Contents: http://scitation.aip.org/content/aip/journal/jcp/140/7?ver=pdfcov
Published by the AIP Publishing

First principles study of the structural, electronic, and transport properties of triarylamine-based nanowires

Akinlolu Akande,[a),b)] Sandip Bhattacharya,[b)] Thomas Cathcart, and Stefano Sanvito
School of Physics, AMBER and CRANN Institute, Trinity College Dublin, Dublin 2, Ireland

(Received 15 August 2013; accepted 27 January 2014; published online 18 February 2014)

We investigate with state of the art density functional theory the structural, electronic, and transport properties of a class of recently synthesized nanostructures based on triarylamine derivatives. First, we consider the single molecule precursors in the gas phase and calculate their static properties, namely (i) the geometrical structure of the neutral and cationic ions, (ii) the electronic structure of the frontier molecular orbitals, and (iii) the ionization potential, hole extraction potential, and internal reorganization energy. This initial study does not evidence any direct correlation between the properties of the individual molecules and their tendency to self-assembly. Subsequently, we investigate the charge transport characteristics of the triarylamine derivatives nanowires, by using Marcus theory. For one derivative we further construct an effective Hamiltonian including intermolecular vibrations and evaluate the mobility from the Kubo formula implemented with Monte Carlo sampling. These two methods, valid respectively in the sequential hopping and polaronic band limit, give us values for the room-temperature mobility in the range 0.1–12 cm^2/Vs. Such estimate confirms the superior transport properties of triarylamine-based nanowires, and make them an attracting materials platform for organic electronics. © *2014 AIP Publishing LLC*. [http://dx.doi.org/10.1063/1.4864754]

I. INTRODUCTION

Triarylamine derivatives are well known to be an excellent hole transporting component used in organic light-emitting diodes (OLEDs).[1] Hence, understanding the behaviour of their radical-cation is crucial for designing efficient materials to be included in optoelectronic devices. Over the past decades, these derivatives have continuously stimulated exciting research both theoretically and experimentally. This is primarily because of the general widespread drive towards incorporating organic semiconductors into modern electronic devices, due to their low cost, low weight, and mechanical flexibility. Two additional advantages of triarylamine derivatives are that they are generally also chemically inert and that their optical and transport properties can be chemically tuned.

It was recently observed by Moulin *et al.*[2] that a number of triarylamine-type molecules self-assemble upon stimulation with light and form one dimensional (1D) nanowires. It was suggested that the self-assembly process involves cooperative phenomena, which begin with the formation of cationic radicals induced by light and then proceed with neutralization upon charge hopping across other molecules. This leads to a supra-molecular polymerization of units that contain a delocalized cationic radical. More recently, the same group used one of those triarylamine-based nanowires as a channel in a two-terminal device setup.[3] They showed that such device exhibits a combination of metal-like transport characteristics and also low interface resistance, although the intrinsic transport properties of the organic nanowires, such as the mobility, were not measured.

In this paper, we report on state of the art density functional theory (DFT) calculations of the structural, electronic, and transport properties of such triarylamine-based nanowires, with the aim of relating the electronic characteristics of the triarylamine precursors to the nanowires charge transport properties. As a byproduct of this analysis we discuss whether or not the electronic properties of the precursors offer sufficient information for understanding the self-assembly process upon illumination. We begin by looking at the derivatives proposed in Ref. 2 in their gas phase and provide a detailed analysis of the electronic structure of these precursors and their intramolecular interactions. As reference material we also include calculations for the basic triphenylamine (TPA) molecule, for which both theoretical and experimental data are available.

We then move to investigating the intermolecular interactions and the transport characteristics of the nanowires. A first estimate of the room-temperature mobility is provided by the semiclassical Marcus theory,[4] which requires the evaluation of the internal reorganization energy and the transfer integrals between molecules dimers. These are all quantities ready available from our electronic structure analysis and so the mobility is estimated for all the triarylamine derivatives. Notably, even though Marcus theory ignores the possibility of coupling to intermolecular phonons and of medium polarization,[5] it has been used to calculate hole mobility in oligothiophenes[6] and pentacene,[7] yielding reasonable values in agreement with experimental trends. Then, for one of the triarylamine derivatives we have used a second approach. This consists in deriving from the *ab initio* calculations an effective Hamiltonian including electron-phonon coupling to

a)Author to whom correspondence should be addressed. Electronic mail: akandea@tcd.ie
b)A. Akande and S. Bhattacharya contributed equally to this work and should be considered as co-first authors.

intermolecular vibrations, and then in extracting the temperature-dependent mobility by linear response Kubo Formula[8] augmented with Monte Carlo sampling. Such second approach is used only for the case of the triarylamine-based nanowires for which experimental transport data are available.[3]

It is important to note here that Marcus theory and the linear response Kubo approach based on an Hamiltonian containing non-local electron-phonon coupling have two different limits of validity. In Marcus theory language, the first is valid when the reorganization energy is much larger than the largest of the hopping integrals, while the second should be considered in the opposite case, i.e., when the reorganization energy can be neglected compared to the hopping integral. Marcus theory then describes hopping conductance, while the second method is designed for band-like transport. As we will see in Sec. III, the nanowires investigated here do not fall in neither of these limiting cases, and in fact for almost all the derivatives the reorganization energy has a similar magnitude than the intermolecular hopping parameter. In such a situation, one expects a crossover between hopping and band-like transport at a certain temperature. This is for instance the case of naphthalene.[9,10]

The paper is organized as follows. In Sec. II, we will briefly describe the system investigated and the computational methods used in this work. Then, in Sec. III, we will present our numerical results together with their discussion, before finally concluding in Sec. IV. More details on how to extract finite temperature charge mobility by Monte Carlo sampling the Kubo formula are presented in the Appendix.

II. SYSTEM AND COMPUTATIONAL METHODS

This study focuses on the set of triarylamine derivatives synthesized in Ref. 2, whose generic structure is shown in Fig. 1. The key difference between the various derivatives is the possibility of choosing the three radicals, R^1, R^2, and R^3. In particular, eight different molecules have been synthesized in Ref. 2 and the same are investigated here. These are listed in Table I. Note that the various molecules are labelled as "precursors" since they are the precursors for the synthesis of the 1D nanowires. The table also indicates whether a particular precursor leads to the actual formation of the nanowire, a process whose unique fingerprint is the disappearance of the NMR signals of the aromatic protons upon exposure to light.[2]

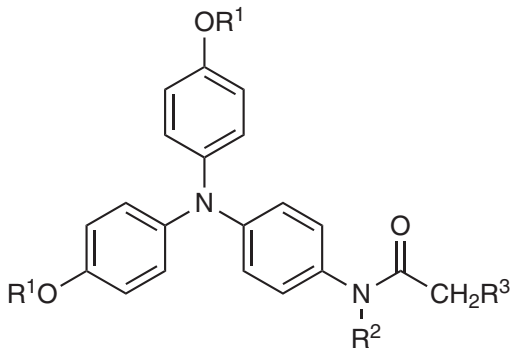

FIG. 1. Structure of the triarylamine derivatives synthesized in Ref. 2 and investigated in this work. R^1, R^2, and R^3 denote the position of three radicals. A list of all the molecules synthesized is provided in Table I.

TABLE I. List of the nanowires precursors synthesized in Ref. 2 and investigated here. The photoactivity is established from the disappearance of the NMR signals of the aromatic protons upon exposure to light. Photo-active precursors lead to the formation of the 1D nanowires. P1 has been highlighted since P1-based nanowires have been employed in the transport experiments of Ref. 3.

Precursor	R^1	R^2	R^3	Photoactive
P1	C_8H_{17}	H	Cl	yes
P2	C_8H_{17}	H	H	yes
P3	C_8H_{17}	CH_3	H	no
P4	C_8H_{17}	H	C_6H_{13}	yes
P5	Bn	H	Cl	yes
P6	Bn	H	H	yes
P7	H	H	Cl	no
P8	CH_3	H	Cl	no

First principles calculations are performed for all the derivatives in the gas phase and for TPA, chosen as a reference system. Since our interest is in hole transport, we restrict the discussion to that of the positively charged derivatives. Their molecular geometry (in the ground and single cationic states), the energy level of the Highest Occupied Molecular Orbital (HOMO) and the Lowest Unoccupied Molecular Orbital (LUMO), the HOMO-LUMO gap, the ionization potential (IP), the total density of states (DOS), and the reorganization energy are computed by using DFT.[11] The B3LYP hybrid functional,[12] which is known to be suitable for most molecular systems is adopted together with a 6-31G* basis set.

In order to evaluate the intermolecular interactions to be input in Marcus theory, we construct molecules dimers from the B3LYP optimized monomers, we calculate their binding energies (BE) and then estimate the transfer integral (TI) as a function of the intermolecular distance along the nanowire axis (z-axis). The mobilities are then computed at the optimum dimer distance (the nanowire lattice parameter), which is at the BE minimum. While B3LYP-DFT usually describes well electronic properties such as the IP, the HOMO-LUMO gap, and molecular geometries, it does not describe in a satisfactory way weak interactions, in particular those of dispersive nature. These include van der Waals (vdW) and π-π interactions, which in turn play an important role in determining the structure of organic materials.[5] As a test, we calculate the BE and TI for the TPA dimer model system by using three additional DFT functionals: the long-range-corrected version of B3LYP (CAM-B3LYP),[14] the meta-hybrid generalized gradiant approximation (GGA) M06-2X functional,[15] and the Grimme's functional including vdW dispersion.[16] Then, by using the functional that returns the lowest BE for TPA, we calculate the BE and TI for all the precursors and estimate the values of their mobilities at the optimal intermolecular distance.

Finally, we move to investigate in detail the charge transport characteristics of such organic nanowires as a function of temperature. DFT calculations are first performed

on a one-dimensional nanowire geometry, by using the optimized B3LYP monomer structure and maintaining the distance between the monomers at that of the BE minimum for the dimer. We then obtain a complete band structure for the organic nanowires and from the dispersion of its valence band we extract an elementary tight-binding Hamiltonian. This includes a static term and a Su-Schrieffer-Heeger-type interaction,[13] which relates the hopping integrals with the molecular displacements in the nanowire, i.e., it introduces electron-lattice coupling. The parameters for such an interaction term are evaluated with a simple finite difference method (see Sec. III C). The charge carrier mobility as a function of temperatures is then calculated by using the linear response Kubo formula, evaluated with Monte Carlo sampling.

Ending this section we report the technical details of the DFT calculations performed in this work. All the simulations for the single molecules in the gas phase are performed with the Gaussian09 suit,[17] using the 6-31G* basis set. The same package is also employed to evaluate the electronic structure of the dimers, then used for the semiclassical Marcus theory. Relaxation with Gaussian09 is carried out with the Berny algorithm[18] until the forces are smaller than 2×10^{-5} Hartrees/Bohrs. After relaxation the phonon spectrum is computed and the vibrational frequencies are inspected. The absence of imaginary frequencies confirms that the energy minima has been reached.

The Quantum Espresso[19] code is used for the electronic structure of the organic nanowires. Spin-polarized DFT calculations are performed at the GGA level as implemented by Perdew, Burke, and Ernzerhof[20] and with the semi-empirical implementation of vdW interactions by Grimme.[16] In all calculations we employ Vanderbilt ultra-soft pseudopotentials.[21] Convergence is tested over the total energy and an accuracy lower than 1 mRy is achieved by a plane wave cut-off 30 Ry. A $5 \times 5 \times 5$ Monkhorst-Pack grid with a Gaussian broadening of 0.01 Ry is used for sampling the reciprocal space. Additional details about our calculations will be provided later on whenever necessary. Also in this case geometrical relaxation is performed by standard conjugate gradient method.

III. RESULTS AND DISCUSSIONS

A. Single molecules in the gas phase

All the precursors and the TPA molecule have been optimized in their neutral and cationic states using the B3LYP hybrid functional. We start our analysis by examining the energy levels of the precursors' frontier molecular orbitals. Table II reports the Kohn-Sham HOMO and LUMO energy levels as well as the HOMO-LUMO gap for all the precursors and TPA. It is clear that, whether light active or not, there is no remarkable difference in the energy levels of the frontier molecular orbitals, meaning that the different radicals that uniquely characterize a given precursor (R^1, R^2, and R^3) have little effect on that region of the quasi-particle spectrum. Note that our calculated values for the TPA (our reference) agree well with existing literature, for instance with those reported in Ref. 22.

Next, we calculate the IP and the hole extraction potential (HEP) of all the precursors. These are important parameters to characterize the molecules hole transport ability. Both IP and HEP are well-defined quantities obtainable by DFT in terms of total energies differences for the molecule in different charging states and positions over the potential energy surface. Thus, the vertical IP, IP(v), is calculated as the energy difference between the neutral molecule and the cationic radical at the geometry of the neutral configuration. Likewise the HEP is the same energy difference, but now calculated at the geometry of the cationic state. Finally, the adiabatic IP, IP(a), is obtained as the energy difference between the neutral and single positively charged state, both calculated at their equilibrium geometries.

The calculated IPs and HEP for all the precursors are shown in Table II. We find the vertical IPs in the range 5.69–6.01 eV, the adiabatic ones in the range 5.54–5.88 eV, while the HEPs distribute over the interval 5.40–5.75 eV. In the case of IP(v), as expected, we find good consistency between our total energy calculations and the Kohn-Sham HOMO levels also reported in Table II, i.e., we find that those precursors showing deep HOMO energies also display a deep IP(v). In particular, the energy order of the various Kohn-Sham HOMOs is the same as that of the IP(v)s. Note that the calculated IP(v)s are not exactly matching the HOMO levels and

TABLE II. DFT-B3LYP estimates of the Kohn-Sham HOMO, ε_H, and LUMO, ε_L, eigenvalues, the HOMO-LUMO gap, $\Delta\varepsilon$, the ionization potentials, IP(v) and IP(a), the hole extraction potential, HEP, the internal reorganization energy, λ_{int}, and the localization radius, d_0, for all the precursors and for TPA. In the case of TPA, the value reported in brackets is the experimental IP from Ref. 25. Note that we report d_0 only for those precursors for which a good exponential fit of the transfer integral as a function of the dimer distance is obtained. We remind here that P3, P7, and P8 are not photo-sensitive, i.e., they do not lead for the nanowires formation.

Precursors	Photoactive	ε_H (eV)	ε_L (eV)	$\Delta\varepsilon$ (eV)	IP(v) (eV)	IP(a) (eV)	HEP (eV)	λ_{int} (eV)	d_0 (Å)
P1	Yes	−4.55	−0.42	4.13	5.81	5.66	5.52	0.30	0.39
P2	Yes	−4.44	−0.23	4.21	5.71	5.57	5.42	0.30	0.38
P3	No	−4.47	−0.20	4.27	5.73	5.57	5.42	0.32	...
P4	Yes	−4.43	−0.22	4.21	5.69	5.54	5.40	0.29	0.44
P5	Yes	−4.64	−0.52	4.12	5.88	5.69	5.52	0.36	0.45
P6	Yes	−4.54	−0.34	4.20	5.79	5.60	5.42	0.37	0.51
P7	No	−4.66	−0.50	4.16	6.01	5.88	5.75	0.26	...
P8	No	−4.60	−0.47	4.13	5.80	5.67	5.53	0.28	0.47
TPA	...	−4.95	−0.30	4.65	6.41(6.88)	6.35		0.12	0.60

that the two differ by about 1 eV, with the quasi-particle energies being systematically more shallow.

In general in DFT, one expects the Kohn-Sham HOMO energy to correspond to the system vertical IP.[26] This condition however is not satisfied by approximated exchange and correlation functionals because of the self-interaction error, and the HOMO levels are usually much more shallow than the true IPs. The B3LYP functional partially removes the self-interaction error. This removal however is not complete and the residual self-interaction is probably responsible for the differences. In any case, the overwhelming result is that there is almost no dependence of the charge extraction energies (IPs and HEP) on the nature of the precursors, meaning that the different radicals have little effect on the ability of a molecule to transfer electrons/holes. Further support to this conclusion is the fact that the IPs for TPA are within 0.5 eV from that of any precursors, indicating that the TPA unit is the molecular block responsible for the charge transfer. Finally, note that our calculated IP value for TPA is not only consistent with other theoretical works[22–24] but also close to the experimental data.[25]

We then examine the DOS of the precursors in their gas phase. Interestingly, the main characteristics of the DOS are qualitatively similar for all the precursors, so that here in Fig. 2 we report only the illustrative case of the P1 molecule (the one for which transport has been measured). The figure reports the DOS for both the neutral state (top panel) and the cation radical (bottom panel), together with the isosurface plots of the charge density of the different molecular orbitals. Note that the results reported here are for GGA, whose only difference from B3LYP for this molecule is in the quantitative position of the energy levels (the order and the symmetry is the same). Note also that in the figure the molecular DOS has been artificially broadened for visualization purposes.

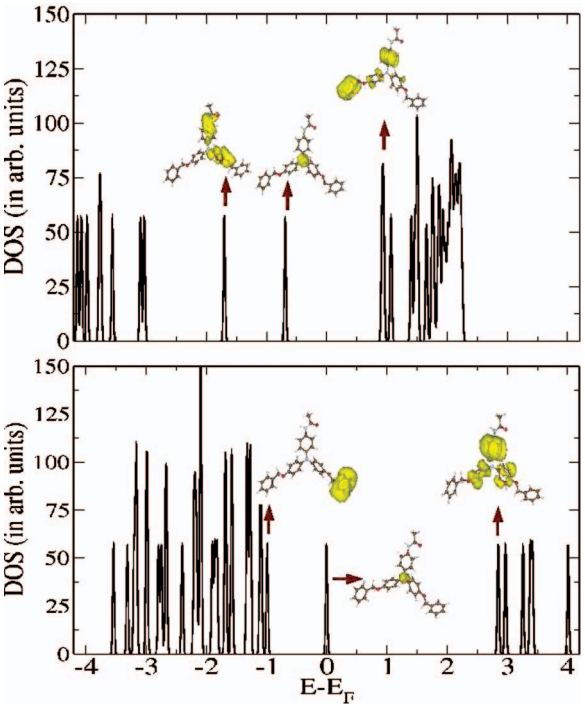

FIG. 2. The DOS of the P1 molecule and the $P1^+$ radical in the gas phase, as calculated from DFT-GGA, are shown in the top and bottom panels, respectively. Charge density isosurfaces (local DOS) for the HOMO−1, HOMO, and LUMO levels are also displayed. The quasi-particle eigenvalues are marked by purple vertical lines, while the DOS has been artificially broadened for visualization purposes (there is no natural broadening). Note that the HOMO of both the neutral molecule and the cation radical have identical symmetry with charge density distribution strongly localized over the N 2*p* orbital of the central TPA unit. The qualitative features of the DOS and the orbitals symmetry of all precursors are very similar.

From the DOS it is clear that the HOMOs of both the neutral molecule and the cationic radical are highly localized on the N atom of the TPA central unit. This means that the ionization process simply involves the extraction of an electron from such double occupied state, without affecting much the rest of the molecule. Indeed a close analysis reveals that the symmetry of the HOMO-1 and of the LUMO is somehow different for the two charging states, indicating level reorganization upon ionization. The same, however, is not true for the HOMO, whose only difference in the two charging states lies in the occupation. In fact, we find that the HOMO of all the precursors investigated here is essentially the same of that of the widely studied TPA isolated molecules,[22,23,27] namely, it is formed by the 2*p* orbitals of the central N ion.

In closing this section, we wish to put our results in the context of the photo-induced self-assembly formation of the nanowires. The mechanism for the nanowires formation proposed in Ref. 2 is that, under exposure to light, initially a small amount of positively charged radical (6 over 1000 molecules) is formed. Our local DOS calculations point out that the positive charge in the radical is localized on the central N atom, as speculated in the original experimental work. According to the mechanism proposed, the positively charged radical comes into contact with a neutral molecule and transfers its charge. This process continues until 1D triarylamines-based bundles of nanowires are formed. Our first principles analysis of the energy levels and of the nature of the frontier molecular orbitals for all the triarylamines derivatives does not provide any evidence that may distinguish the light active precursors (which self-assemble into supra-molecular organic nanowires) from those, which are not light active. In other words, we do not find any fingerprint in the electronic structure of the precursors, which can help us to identify the conditions for the self-assembly. Thus, we conclude that the self-assembly process may be initiated by factors not completely intrinsic to the molecular precursors. For example, it may affected by the strength of the oxidizing agent used in the solvent, i.e., by the interaction of the different precursors with the solvent.

B. Charge transport properties from Marcus theory

In the weak coupling limit, charge transfer between molecules is described by Marcus theory,[4] and the calculated charge transfer rates can be used for evaluating the mobility of molecular crystals. Under the assumption that the temperature is sufficiently high so that vibrations can be treated classically, Marcus' formula for the hole transfer rate, K_{CT}, reads[4]

$$K_{CT} = \left(\frac{\pi}{\lambda k_B T}\right)^{1/2} \frac{J^2}{\hbar} \exp\left(-\frac{\lambda}{4k_B T}\right), \qquad (1)$$

where T is the temperature and k_B is the Boltzmann constant. In Eq. (1), the two materials-specific quantities are the charge reorganization energy, λ, and the transfer integral, J. Various approaches have been put forward in literature to estimate these parameters (see, for instance, Ref. 28).

The most popular method for evaluating the transfer integrals for a hole transporting pair of identical molecules is rooted in Koopmans' theorem,[29] which establishes that the HOMO of the neutral molecule is the negative of the ionization potential. This, together with the assumption that the geometry of the ground state of the neutral molecule is a good approximation of the geometry at the point of charge transfer,[30] allows one to evaluate the absolute value of the transfer integral, $|J|$, as half of the energy difference between the HOMO and HOMO-1 levels of a dimer of molecules in its closed-shell configuration. In practice the idea is that, in the weak coupling limit, the energy separation between the HOMO and HOMO-1 levels of the dimer is simply the energy split between the bonding and anti-bonding orbitals derived from the HOMO of the individual molecule. This quantity is largely kinetic and as such it should be relatively independent on the actual position of the HOMO level, i.e., on how the specific exchange and correlation functional reproduces a correct quasi-particle spectrum. In other words, one expects that it should not be important how a particular exchange and correlation functional quantitatively satisfies Koopmans' theorem as long as different functionals return the same HOMO, i.e., that the transfer integrals are calculated for the same molecular orbitals. Because of its simplicity this approach has been widely used in the literature to estimate J for organic molecules,[5,30–33] although caution should be taken when the dimer is not co-facially stacked[34] and corrections should be included.[35]

The reorganization energy deserves additional discussion. This contains two parts, namely, an internal, λ_{int}, and an external, λ_{ext}, one. The internal contribution is intrinsic of the two molecules exchanging charge and accounts for the change in molecular geometry corresponding to the charge transfer, i.e., it accounts for the different geometries of the molecule in different charging states. In contrast, λ_{ext} describes the change in electronic polarization of the surrounding molecules associated with the charge transfer process. Such external contribution is not straightforward to calculate.[28] However, for molecular crystals λ_{ext} is usually neglected since it is considerably smaller than λ_{int}.[33] The internal reorganization energy can then be written as the sum of two terms:[35] (1) the difference between the total energy of the neutral precursor at its equilibrium geometry and that at the geometry of the radical ion, and (2) the difference between the energy of the radical ion at its equilibrium geometry and that at the geometry of the neutral configuration. By taking the definitions introduced before we can write

$$\lambda_{int} = \mathrm{IP(v)} - \mathrm{HEP}\,. \tag{2}$$

Since both IP and HEP for all the precursors are similar, we do not expect λ_{int} to differ much across the various precursors, as demonstrated in Table II. Also for this quantity our calculated value for TPA compares well with those reported in previous works.[22–24]

Let us now move to computing the J's. First, we need to calculate the equilibrium separation, d_{eq}, of the various dimers, i.e., to compute the dimer BE as a function of the separation, d, between two identical monomers. The geometry of each molecule in the dimer is optimized by using the B3LYP hybrid functional and the 6-31G* basis set, and the dimer considered in this work has a co-facial orientation. This means that the planes defined by the three bonds proceeding from the central N atom on each molecule are parallel to each other, with the two N atoms situated on a vector normal to their planes. This simulates a wire in which the central N atoms of the TPA unit are co-axial. Even though J may strongly depend on the type of crystal packing, the co-facial orientation is usually considered as a geometry of interest, having a high symmetry reference point and being an upper limit for the electronic coupling.[37] Furthermore, a geometry of this type has been suggested for the nanowires under investigation by our reference experiments.[2,3]

Note that, in the weak coupling limit, one expects the J's to vary exponentially with d,[30]

$$|J| \sim \exp(-d/d_0)\,, \tag{3}$$

where d_0 is a constant called the localization radius. This decay is well understood and attributed to the exponential decay of the intermolecular overlap between the orbitals when the two monomers are pulled apart. In our analysis, we will test such property, by starting with the case of TPA.

The BE and the transfer integral of TPA calculated by using different DFT functionals are presented in Fig. 3. We note here that the BE is obtained by neglecting the basis set superposition error, since it has a negligible contribution.[36] We first determine the dimer optimum distance and then we examine

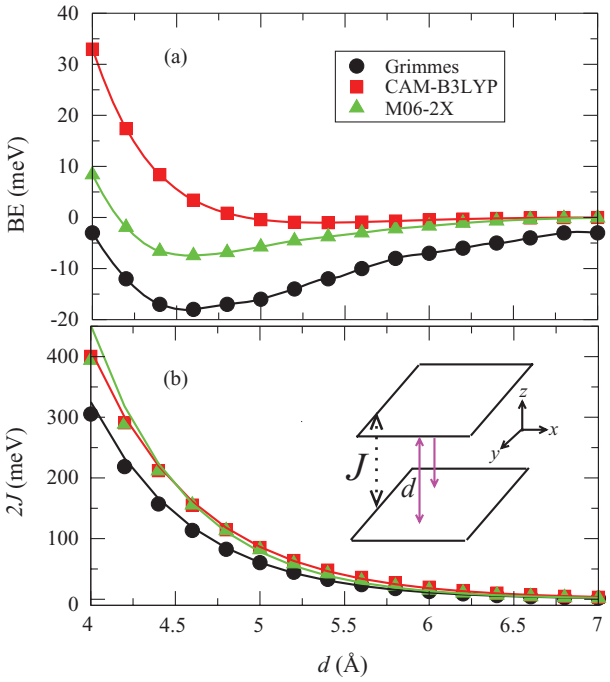

FIG. 3. Variation of the (a) binding energy, BE and of the (b) charge transfer integral of TPA calculated by using different DFT functionals. The solid line in (b) is exponential fits of the data.

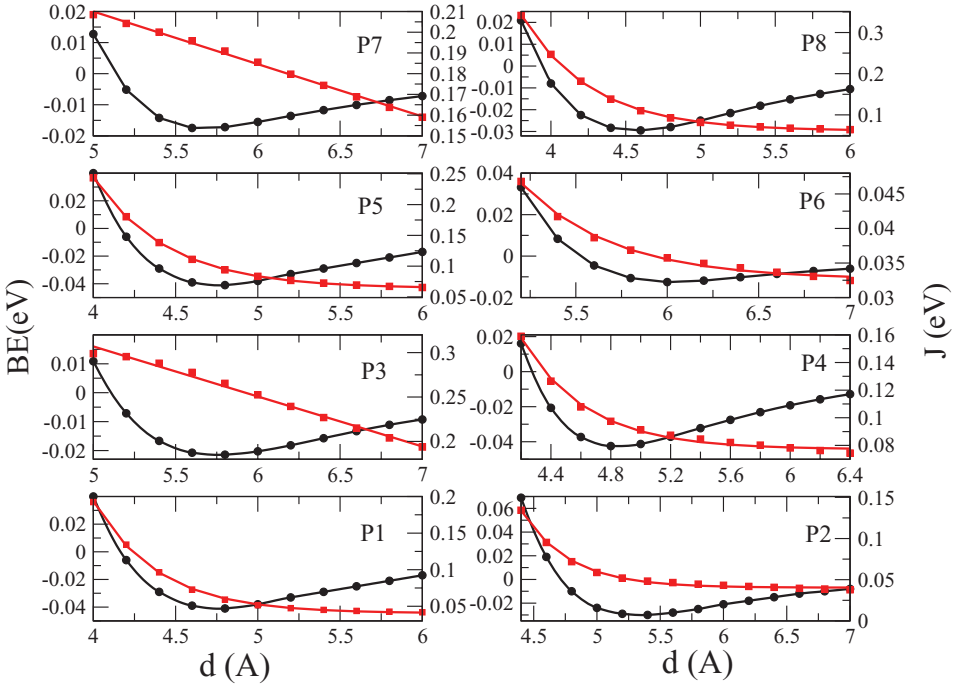

FIG. 4. Binding energy (solid circles and left-hand side vertical axis) and charge transfer integrals (open squares and right-hand side vertical axis) for all the precursors calculated at the geometry provided by the Grimme's functional. The solid black lines interpolate the binding energies, while the red dashed lines are an exponential fit of the transfer integrals.

J around this region. As expected *J* decays exponentially with *d* with the values of d_0 being 0.60 Å, 0.64 Å, and 0.57 Å, when the BE is evaluated respectively with the Grimme, the CAM-B3LYP, and the M06-2X functionals. The figure shows that only Grimme and M06-2X bind the dimer, while for CAM-B3LYP the binding energy does not present a minimum with *d*. Furthermore, we notice that although the equilibrium intermolecular distance is predicted rather consistently for the two functional, Grimme displays a significantly larger binding energy that M06-2X. This is in virtue of the explicit inclusion in Grimme of pairwise van der Waals interactions. With these considerations at hand we have decided to optimize the dimer intermolecular distance for all the precursors by using the Grimme functionals. However, we then calculate the TI's by using both the Grimme and the B3LYP functional (at the geometry obtained with Grimme), so that we can compare results from functionals that satisfy the Koopmans theorem at a different level of accuracy.

As for the TPA, also for all the nanowires precursors we consider a co-facial arrangement of the dimers. We note that performing a rotation of one of the two molecules in the dimer around the axis joining the two N atoms gives approximately the same binding energy as that of a perfectly co-facial geometry. This further supports the idea that the co-facial geometry is indeed representative for the charge transfer, which interests by large the N atoms only. In Fig. 4, we present the BE and *J*'s as a function of the N-N distance for all the precursors. Clearly in all cases, the dimer can form and one can identify an equilibrium intermolecular distance. This is true also for P3, P7, and P8, that experimentally are found not to be photo-sensitive, i.e., they do not lead to the nanowires formation.

Moving to the *J*'s we notice that for all photo-sensitive precursors (P1, P2, P4, P5, and P6) there is a clear exponential decay of *J* as a function of the dimer intermolecular separation, while this is not the case for the non-photo-sensitive ones (P3 and P7), for which the decay is linear. The precursor P8 remains outside this picture, since it is not photo-sensitive and yet the decay of *J* is exponential. As such, also the transfer integrals do not seem to provide a clear way to differentiate photo-sensitive from non-photo-sensitive precursors. Finally, in Table III, our estimated *J* values calculated at the minimum of the BE (Grimme) are tabulated for all the precursors using the Kohn-Sham spectrum obtained either with the Grimme or the B3LYP functional. Notably there is a rather good agreement between the two functionals, strengthening the argument made before about the kinetic nature of the transfer integrals. Intriguingly, we find the largest three transfer integrals for the

TABLE III. Table comparing the estimated *J* values at the minimum of the BE calculated by using the Grimme and the B3LYP functional for all the precursors. Note that in both cases the dimer optimal geometry and d_{eq} are that obtained with Grimme, since B3LYP does not bind the dimer.

Precursors	d_{eq} (Å)	J_{Grimme} (meV)	J_{B3LYP} (meV)	μ (cm^2/Vs)
P1	4.8	29.54	34.03	0.13
P2	5.4	24.18	24.61	0.11
P3	5.8	132.68	134.25	3.10
P4	4.8	48.72	51.88	0.40
P5	4.8	46.99	53.92	0.17
P6	6.0	17.86	18.14	0.04
P7	5.6	97.93	99.06	3.11
P8	4.6	55.05	64.31	0.53

three precursors known not to form nanowires, while the values for all the others are rather similar ranging from ∼18 meV to ∼50 meV. Importantly, we do not find any particular correlation between the equilibrium dimer intermolecular separation, d_{eq}, and the magnitude of the transfer integral, apart for P6, which has the smallest J and the largest d_{eq}. This indicates that the fine details of the electronic structure of the precursors determine the molecule ability to exchange charges.

Finally, we are now in the position of evaluating the nanowires mobilities. If one neglects *extrinsic* effects, the charge carrier mobility, μ, can be estimated by using the following expression:[28,38]

$$\mu = \frac{e}{k_B T} d_{eq}^2 K_{CT} , \quad (4)$$

where e is electron charge. Having calculated both the λ_{int}'s (Table II) and the J's (Table III) for all the precursors, the estimated mobilities at room temperature (300 K) are reported in Table III. Notably, with the exception of P3 and P7, which anyway do not form, the mobilities are all around some fraction of cm^2/Vs, with the maximum value being for P4 (0.40 cm^2/Vs) and the minimum for P6 (0.04 cm^2/Vs). Such similarity between the mobilities is expected in the light of the fact that the transport occurs through the central N atom of the TPA unit, i.e., through a molecular orbital common to all precursors and largely independent from the particular radicals which characterize the precursors. This reflects in similar reorganization energies and, although to a smaller degree, transfer integrals, and therefore in similar mobilities.

C. Charge transport properties from linear response theory

As an alternative to Marcus theory, valid for band-like transport, we now revaluate the mobility of P1 by linear response theory with parameters extracted from DFT. The first task consists in writing an adequate tight-binding Hamiltonian for the nanowires including electron-phonon coupling to a few relevant vibrational modes. We begin by calculating the electronic structure of the nanowires. This is obtained by placing a single molecule, whose geometry has been optimized by DFT-B3LYP (the same of Sec. III B), in an orthorhombic unit cell with lattice parameters a, b, and c. In particular, we take c as the intermolecular separation for the dimer calculated in Sec. III B and $a, b \gg c$ (see Table III). We verify that further crystal relaxation does not change significantly the value of c (the exchange and correlation functionals used to optimize the dimers and the 1D nanowires are the same), while considering $a = b = 63.5$ Å ensures that there is no interaction between the image cells in the plane, i.e., that there is no interaction between adjacent nanowires. The spin-polarized DFT calculations are performed with Quantum Espresso and the Grimme's exchange correlation functional[16] and the internal coordinates of atoms inside the unit cell are relaxed until the forces are smaller than 10^{-4} Ry/Å.

Note that the electronic structure of the nanowires is calculated for the individual molecules in a neutral configuration, so that the wires are in an insulating state and do not develop Peierls distortion. Actual samples, however, are hole doped

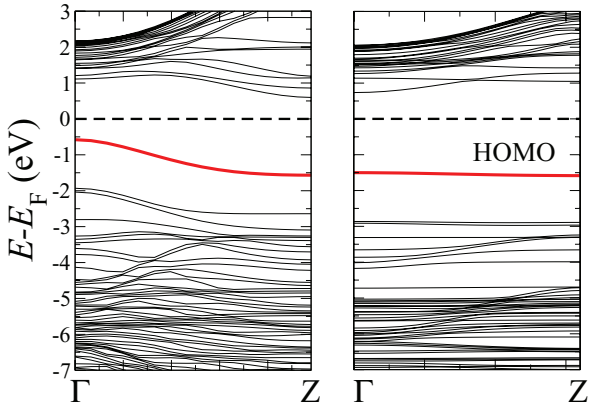

FIG. 5. Bandstructure of a nanowire obtained by repeating periodically the P1 unit, plotted over the 1D Brillouin zone. Here we present data for the equilibrium lattice parameter $c = d_{eq} = 4.8$ Å (right panel) and for a strongly compressed structure $c = 3.18$ Å (left panel). The nanowire geometry keeps the molecules in a co-facial arrangement and the distance between the N centers is the same equilibrium distance found for the corresponding dimer (see Table III). A single-orbital per site tight-binding Hamiltonian, where the relevant orbital is the HOMO, can be extracted from the bandstructure by fitting the HOMO-derived band (in red). The dashed horizontal line denotes the Fermi level, which is simply placed in the HOMO-LUMO gap.

so that one, in principle, can expect a Peierls-distorted ground state geometry. This is likely not to be relevant for the finite temperature mobility except at very low temperatures. In fact, the hole concentration inferred from the experiments is rather low (six cations every 1000 molecules[2]), well below half-filling, so that the Peierls distortion wavelength is long and the associated energy gain is small. As a consequence, we expect that Peierls distortion may play a role in these nanowires only at rather low temperatures, a regime not investigated here.

Fig. 5 displays the bandstructure of the nanowire constructed from the P1 molecules (henceforth referred to as the nanowire P1) plotted along the 1D Brillouin zone, $\Gamma - Z$. In the figure, we report data for c being the equilibrium lattice constant, $d_{eq} = 4.8$ Å, and for an extremely compressed configuration, where $c = 3.18$ Å. This allows us to trace the bandstructure as the lattice parameter changes. Importantly, we find that the band relative to the HOMO is always well separated from the rest of the valence manifold even at the compressed lattice parameter. This means that there is little interaction among the HOMO-derived band and the rest of the valence, so that a single-site tight-binding effective Hamiltonian appears appropriate for the problem of hole conduction. A different situation appears for the conduction part of the bandstructure, which is characterized by a number of closely spaced bands presenting crossing.

In any case, we map the HOMO-related band onto the following tight-binding Hamiltonian

$$\hat{H}_{HOMO} = \sum_{ij} [t_{ij} + \alpha(q_i - q_j)](c_i^\dagger c_j + h.c.) + \sum_{ij} \frac{1}{2} K (q_i - q_j)^2 , \quad (5)$$

where $t_{ij} = t$ denotes the hopping integral between the molecules in the wire and extends only to nearest-neighbour

molecules, α is the carrier-phonon coupling, and K is the stiffness constant. Here $c_i^\dagger$ (c_i) is the creation (annihilation) operator for a charge carrier at the ith site (molecule), while q_i is a classical vector describing the displacement of the ith molecule of the nanowire from its equilibrium position.

The magnitudes of the hopping integrals, t, can be simply obtained from the dispersion of the HOMO-derived band (Fig. 5) as $t = \Delta/4$, where Δ is the bandwidth. For the P1 nanowire at $c = d_{eq}$ (right panel Fig. 5), we extract $t = 25.0$ meV, which is in close agreement with the value calculated for the corresponding dimer (29.5 meV from Table III).

The parameters of H_{HOMO} related to the coupling to the vibrations, namely α and K, can be evaluated from finite difference. In practice, we displace the molecule along a particular direction $\mathbf{r}$ (the phonon mode displacement vector) and then compute $\alpha_{\hat{r}} = \frac{\delta t}{\delta \mathbf{r}}$ and $K = \frac{1}{\mathbf{r}} \frac{\delta E}{\delta \mathbf{r}}$, where E is the DFT total energy. In order to estimate the mobility we consider a single acoustic phonon mode constructed by displacing the molecules along the nanowire axis with respect to each other. This is illustrated in Fig. 6 and referred to as the C-I mode. We expect such particular phonon mode to be the most significant in governing charge transport through the organic nanowire. In fact, the motion of the molecules along the nanowire axis facilitates the overlap between the density of the localized carriers thereby enhancing the charge transfer, a mechanism proposed in the original experimental work[2] to justify the excellent transport properties measured. For the P1 nanowire and the C-I mode we obtain $\alpha/t = 1.585$ 1/Å and $K/t = 1.530$ 1/Å^2.

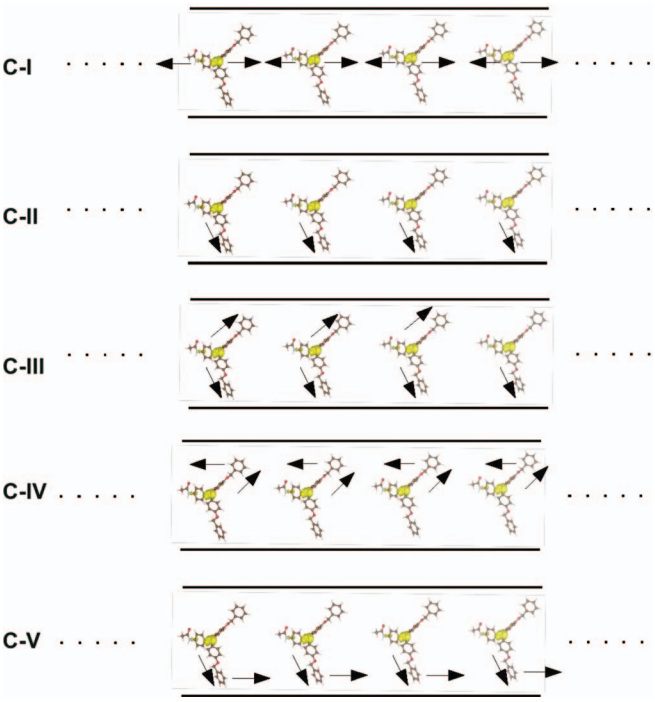

FIG. 6. Schematic illustration of the molecular displacement of the different phonon modes for which the carrier-phonon coupling, α, and the stiffness constants, K, have been calculated. The picture is for the P1 nanowire. The various modes are labelled as C-I to C-V and only the C-I mode is considered when estimating the charge carrier mobility.

TABLE IV. Table showing the calculated values for α/t along the various phonon modes for the P1 nanowire. The labels for the phonons are those introduced in Fig. 6. In the table, we also report the result for the rubrene crystal[40] as reference.

Mode	α/t (1/Å)
C-I	1.585
C-II	0.000
C-III	0.067
C-IV	0.501
C-V	0.370
Rubrene	0.047

Together with the C-I mode we have also evaluated α/t for other relative molecular displacements, as depicted in Fig. 6 (C-II to C-V). The results are listed in Table IV. In the same table, we report as a comparison also α/t for the mode most relevant to the longitudinal transport in rubrene,[40] the organic crystal displaying the overall highest mobility. In general, we find the electron-lattice coupling along the C-I displacement to be significantly larger than that of all the others, and also of the analogous longitudinal mode in rubrene. This justifies our approximation of considering only the C-I mode when evaluating the mobility. It also tells us that the electron-lattice coupling in such nanowires is strong so that the mobility should display a rather strong temperature dependence.

We finally turn our attention to the mobility. This is calculated as a function of temperature using the linear response Kubo formula evaluated over a Monte Carlo sampling. The dynamical quantities entering the Monte Carlo scheme are the longitudinal displacements of the molecules (tight-binding sites), which are treated as a continuous variable.[39] After equilibration the charge carrier mobility is evaluated using the Kubo formula[8] averaged over 100 000 Monte Carlo configurations. For a detailed description on how to evaluate the charge carrier mobility for a particular Monte Carlo configuration we refer the reader to the Appendix.

Fig. 7 shows the statistical distributions of the transfer integral $t + \alpha(q_i - q_j)$ evaluated both at low and high

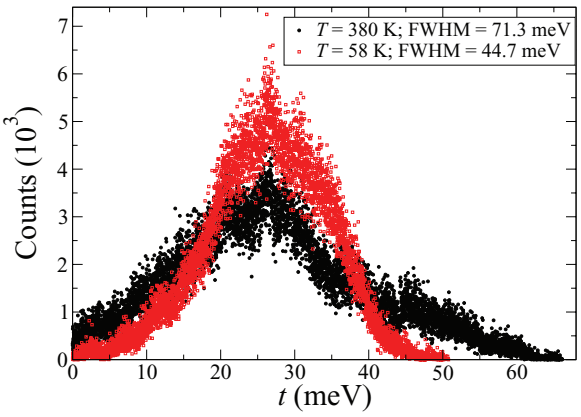

FIG. 7. The statistical distributions of the transfer integral $t + \alpha(q_i - q_j)$ are shown at two different temperatures. The distributions are obtained from Monte Carlo simulations. For both temperatures the transfer integral fluctuates by about 100% of its magnitude as a result of the large value of α obtained for the phonon mode C-I.

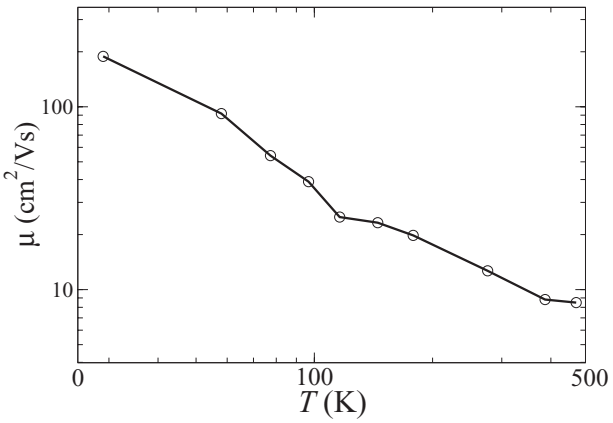

FIG. 8. Our *ab initio* estimate for charge carrier mobility, μ, as a function of temperature for the P1 nanowire. The mobility drops drastically with temperature (note the double logarithmic scale) as a consequence of the very large value of carrier-phonon coupling calculated. At room temperature ($T = 300$ K) the mobility is found to be 11.6 cm^2/Vs.

temperature. As expected the fluctuations in the transfer integrals are larger at a higher temperature. This can be quantitatively observed in the full width at half maxima (FWHM) of the distribution, which is 71.3 meV and 44.7 meV, respectively, at 380 K and 58 K. Also important is to note that, based on the statistics, the fluctuation in the hopping integral is almost 100% of the static value at both temperatures. Such large fluctuations observed in the hopping integral are also fingerprint of the fact that the transport in these nanowires is dominated by dynamic disorder.[41,42] In this limit charge localization over a general band-like transport is created as the result of large fluctuations of the charge transfer integral.

Finally, Fig. 8 shows the calculated mobility, μ, of the P1 nanowire as a function of temperature. We find an extremely severe dependence of μ over T, which is evident in its reduction by almost two orders of magnitude when T goes from 10 K to 500 K (note the double logarithmic scale). This is due to the rather strong carrier-phonon coupling, together with a general softness of the nanowires. Note in fact that here $K = 0.03825$ eV/Å^2, while for the longitudinal mode of rubrene one has $K = 0.06612$ eV/Å^2.[40] Therefore it appears that, along the most relevant vibrational modes, the P1 nanowire appears to be significantly softer than rubrene. Our results thus point to a transport mechanism dominated at high temperature by dynamic disorder,[41,42] where the degree of charge localization increases with temperature, as expected by an increasing spread of the statistical distribution of the hopping parameters. At $T = 300$ K, we estimate a charge carrier mobility of 11.6 cm^2/Vs. This is a rather large value for any one-dimensional object (except for carbon nanotubes). Thus our theoretical analysis confirms the experimental results, which attribute to the nanowires exceptional charge transport properties.

In concluding this section, it is important to note that for the P1 nanowire the room temperature mobility evaluated from Marcus theory and that calculated from linear response with non-local electron-phonon coupling differ by two orders of magnitude, with the former being the smaller. This is not surprising since the two theories are applicable in rather different limits, namely, hopping and band-like transport. As mentioned before the fact that the reorganization energy is comparable to the hopping integral does not allow us to conclude with certainly in favour of any of the two transport mechanisms, and in fact it is likely that in actual nanowires there is a crossover between the two regimes as the temperature increases, similarly naphthalene.[9,10] In principle, such crossover temperature can be calculated, by refining our model to include both local and non-local phonons. This will however require extremely detailed information on the phonon structure of the nanowires, which in turn requires an accurate knowledge of their crystal structure. Unfortunately, such a knowledge is not available to us. By using the learning acquired with naphthalene we speculate that the room-temperature behaviour of the nanowires is likely to be hopping-like. However, providing that we do not know the crossover temperature between the two regimes, a conservative estimate positions the mobility in between that obtained by Marcus theory (assuming hopping conduction up to room temperature) and that calculated with the Kubo approach and non-local phonons (neglecting local vibrations).

IV. CONCLUSIONS

We have reported on a detailed first principles study of the structural, electronic, and transport properties of a class of triarylamine derivatives recently synthesized.[2] Our aim was that of gaining insights in the self-assembly process leading to 1D nanowires and in the charge transport characteristics of such nanowires. The basic electronic structure of the molecules in the gas phase is rather similar for all the precursors with a HOMO mainly localized around the N atom of the triarylamine unit. As a consequence, all the precursors appear to have rather similar ionization potentials. These first calculations suggest that the criterion for the formation of supramolecular self-assembled organic nanowires in triarylamine derivatives is independent of the precursor chemistry.

Next the electron transport properties of the nanowire are explored. First, we evaluate the hole mobilities of all the precursors by using Marcus theory, with the transfer integrals evaluated from the electronic structure of molecular dimers and the reorganization energy from the ionization potential of the single molecules. Then, for the P1 precursors, we also perform linear response mobility calculations by considering the most relevant phonon mode. As expected we find the mobility calculated from Marcus theory to be about two orders of magnitude smaller than that extracted from linear response, which reaches 12 cm^2/Vs at room temperature. These two values can be realistically taken as the lower and upper bonds for the nanowire mobility. Our results thus prove that triarylamine-based nanowires are indeed good hole conductors. Their ability to self-assembly *in situ* in a device geometry[3] makes them interesting candidates for organic electronics devices.

ACKNOWLEDGMENTS

The authors are grateful to Graeme Watson for advising on the use of the Gaussian09 package. This work is supported by Science Foundation of Ireland under the Grant No.

07/IN.1/I945 and the CSET grant underpinning CRANN. Additional funding has been provided by the European Research Council under the European Union's Seventh Framework Programme (FP/2007-2013)/ERC Grant Agreement No. 307891. T.C. acknowledges the Irish Research Council for financial support. Computational resources have been provided by the HEA IITAC project managed by the Trinity Center for High Performance Computing.

APPENDIX: CHARGE-CARRIER MOBILITY FROM KUBO'S FORMULA

The frequency, ω, dependent conductivity calculated in the diffusive limit for a Monte Carlo configuration characterized by the set of atomic displacements $\{q_i\}$ is given by the Kubo's linear response formula

$$\mathrm{Re}[\sigma(\omega;\{q_i\})] = \frac{(ea)^2}{\hbar}\frac{2\pi}{V\omega}\sum_{\lambda,\lambda'}(f_\lambda - f_{\lambda'})|\langle\lambda|J|\lambda'\rangle|^2 \times \delta(E_\lambda - E_{\lambda'} + \omega)\,, \tag{A1}$$

where f_λ is the Fermi function for the carrier eigenstate with quantum number λ and energy E_λ,

$$f_\lambda = \frac{1}{\exp[(E_\lambda - \mu_o)/k_\mathrm{B}T] + 1}\,. \tag{A2}$$

In Eqs. (A1) and (A2) e is the electronic charge, a is the equilibrium distance between neighbouring sites (molecules), $V = La$ is the system volume with L being the length of the nanowire and μ_o is the chemical potential. The matrix elements in Eq. (A1) are those of the current-correlation operator, which can be rewritten in terms of the unitary matrix U which diagonalizes H_HOMO (Eq. (5)),

$$\langle\lambda|J|\lambda'\rangle = \sum_{ij}\tau_{ij}[U(i,\lambda)U(j,\lambda') - U(j,\lambda)U(i,\lambda')]\,. \tag{A3}$$

Here $\tau_{ij} = t_{ij} + \alpha(q_i - q_j)$. Finally, the δ-function can be written as a Lorentzian with broadening η ($\eta \to 0$),

$$\delta(E_\lambda - E_{\lambda'} + \omega) = \frac{\pi\eta}{(E_\lambda - E_{\lambda'} + \omega)^2 + (\eta)^2}\,. \tag{A4}$$

Thus the charge-carrier mobility of a particular configuration, μ_i, can be written as

$$\mu_i = \frac{1}{\rho e}\lim_{\omega\to 0}\mathrm{Re}[\sigma(\omega;\{q_i\})]\,, \tag{A5}$$

where ρ is the carrier density. In the calculations presented here we emulate an organic field effect transistor setup with low carrier density ($\rho = 1/L$).

The final mobility, μ, is the average of all the μ_i calculated at the molecular displacements generated by the Monte Carlo scheme,[39] after it has reached equilibrium.

[1]For a review see Z. Ning and H. Tian, Chem. Commun. **2009**, 5483.
[2]E. Moulin, F. Niess, M. Maaloum, E. Buhler, I. Nyrkova, and N. Giuseppone, Angew. Chem. Int. Ed. **49**, 6974 (2010).
[3]V. Faramarzi, F. Niess, E. Moulin, M. Maaloum, J.-F. Dayen, J.-B. Beaufrand, S. Zanettini, B. Doudin, and N. Giuseppone, Nat. Chem. **4**, 485 (2012).
[4]R. A. Marcus, J. Chem. Phys. **24**, 966 (1956); Rev. Mod. Phys. **65**, 599 (1993).
[5]G. R. Hutchison, M. A. Ratner, and T. J. Marks, J. Am. Chem. Soc. **127**, 16866 (2005).
[6]G. R. Hutchison, M. A. Ratner, and T. J. Marks, J. Am. Chem. Soc. **127**, 2339 (2005).
[7]W.-Q. Deng and W. A. Goddard III, J. Phys. Chem. B **108**, 8614 (2004).
[8]G. D. Mahan, *Many-Particle Physics* (Kluwer Academic/Plenum Publishers, 1981).
[9]L. B. Schein, C. B. Duke, and A. R. McGhie, Phys. Rev. Lett. **40**, 197 (1978).
[10]N. Karl, Synth. Metals **133–134**, 649 (2003).
[11]P. Hohenberg and W. Kohn, Phys. Rev. **136**, B864 (1964); W. Kohn and L. J. Sham, *ibid.* **140**, A1133 (1965).
[12]C. Lee, W. Yang, and R. G. Parr, Phys. Rev. B **37**, 785 (1988); A. D. Becke, J. Chem. Phys. **98**, 5648 (1993).
[13]W. P. Su, J. R. Schrieffer, and A. J. Heeger, Phys. Rev. Lett. **42**, 1698 (1979); Phys. Rev. B **22**, 2099 (1980).
[14]T. Yanai, D. Tew, and N. Handy, Chem. Phys. Lett. **393**, 51 (2004).
[15]Y. Zhao and D. G. Truhlar, Theor. Chem. Acc. **120**, 215 (2008).
[16]S. Grimme, J. Comput. Chem. **27**, 1787 (2006).
[17]M. J. Frisch, G. W. Trucks, H. B. Schlegel *et al.*, Gaussian 09, Revision A.01, Gaussian Inc., Wallingford, CT, 2009.
[18]X. Li and M. J. Frisch, J. Chem. Theory Comput. **2**, 835 (2006).
[19]P. Giannozzi, S. Baroni, N. Bonini, M. Calandra, R. Car, C. Cavazzoni, D. Ceresoli, G. L. Chiarotti, M. Cococcioni, I. Dabo, A. Dal Corso, S. de Gironcoli, S. Fabris, G. Fratesi, R. Gebauer, U. Gerstmann, C. Gougoussis, A. Kokalj, M. Lazzeri, L. Martin-Samos, N. Marzari, F. Mauri, R. Mazzarello, S. Paolini, A. Pasquarello, L. Paulatto, C. Sbraccia, S. Scandolo, G. Sclauzero, A. P. Seitsonen, A. Smogunov, P. Umari, and R. M. Wentzcovitch, J. Phys.: Condens. Matter **21**, 395502 (2009).
[20]J. P. Perdew, K. Burke, and M. Ernzerhof, Phys. Rev. Lett. **77**, 3865 (1996).
[21]D. Vanderbilt, Phys. Rev. B **41**, 7892 (1990).
[22]B. Yang, S.-K. Kim, H. Xu, Y.-I. Park, H. Zhang, C. Gu, F. Shen, C. Wang, D. Liu, X. Liu, M. Hanif, S. Tang, W. Li, F. Li, J. Shen, J. W. Park, and Y. Ma, ChemPhysChem **9**, 2601 (2008).
[23]B. C. Lin, C. P. Cheng, and Z. P. M. Lao, J. Phys. Chem. A **107**, 5241 (2003).
[24]M. Malagoli and J. L. Brédas, Chem. Phys. Lett. **327**, 13 (2000).
[25]G. Meijer, G. Berden, W. L. Meerts, H. Hunziker, M. S. deVries, and H. R. Wendt, Chem. Phys. **163**, 209 (1992).
[26]J. F. Janak, Phys. Rev. B **18**, 7165 (1978); J. P. Perdew, R. G. Parr, M. Levy, and J. L. Balduz, Phys. Rev. Lett. **49**, 1691 (1982); J. P. Perdew and M. Levy, *ibid.* **51**, 1884 (1983).
[27]B.-C. Wang, H.-R. Liao, J.-C. Chang, L. Chen, and J.-T. Yeh, J. Lumin. **124**, 333 (2007).
[28]Z. Shuai, L. Wang, and C. Song, *Theory of Charge Transport in Carbon Electronic Materials* (Springer, 2012).
[29]T. Koopmans, Physica **1**, 104 (1934).
[30]J. Kirkpatrick and J. Nelson, J. Chem. Phys. **123**, 084703 (2005).
[31]J. L. Brédas, D. Beljonne, V. Coropceanu, and J. Cornil, Chem. Rev. **104**, 4971 (2004).
[32]B. C. Lin, C. P. Cheng, Z. Q. You, and C. P. Hsu, J. Am. Chem. Soc. **127**, 66 (2005).
[33]X.-K. Chen, L.-Y. Zou, A.-M. Ren, and J.-X. Fan, Phys. Chem. Chem. Phys. **13**, 19490 (2011).
[34]E. F. Valeev, V. Coropceanu, D. A. da Silva Filho, S. Salman, and J. L. Brédas, J. Am. Chem. Soc. **128**, 9882 (2006).
[35]X. Yang, Q. Li, and Z. Shuai, Nanotechnology **18**, 424029 (2007).
[36]S. Kwon, K.-R. Wee, J. W. Kim, C. Pac, and S. O. Kang, J. Chem. Phys. **136**, 204706 (2012).
[37]V. Coropceanu, J. Cornil, D. A. da Silva Filho, Y. Olivier, R. Silbey, and J. L. Brédas, Chem. Rev. **107**, 926 (2007).
[38]M. Pope and C. E. Swenberg, *Electronic Processes in Organic Crystals and Polymers* (Oxford University Press, New York, 1999).
[39]S. Bhattacharya, M. S. Ferreira, and S. Sanvito, J. Phys.: Condens. Matter **23**, 316001 (2011).
[40]S. Bhattacharya and S. Sanvito, "*Ab initio* estimation of spin and charge transport properties of rubrene using maximally localized Wannier functions," Phys. Rev. B (unpublished).
[41]A. Troisi and G. Orlandi, Phys. Rev. Lett. **96**, 086601 (2006).
[42]A. Troisi, Adv. Mat. **19**, 2000 (2007).